

# ON COMPUTABILITY AND ERROR CONTROL IN CFD

CLAES JOHNSON

*Mathematics Department, Chalmers University of Technology, 41296 Göteborg, Sweden*

## SUMMARY

We give an overview of some recent results concerning quantitative adaptive error control in CFD.

KEY WORDS: adaptivity; error control; computability; CFD; fluid flow

## 1. INTRODUCTION

Adaptive error control in CFD concerns the fundamental problem of computability of fluid flow. A flow is computable with a given amount of computational power if a sufficiently accurate solution can be computed solving the Navier–Stokes equations numerically using a computer. Fluid flow may be complex with the complexity and computational difficulty in general increasing with increasing Reynolds number.

Adaptive error control aims at automatically controlling the discretization error for a given problem in a given norm on a given tolerance level. Ideally the error control should be (i) reliable in the sense that the desired error control is guaranteed and (ii) efficient in the sense that the required computational work is close to minimal. Adaptive error control and computability are intimately coupled because (i) reliable quantitative error control is required to verify computability and (ii) efficient use of computational resources is required if limits of computability are touched.

It is a surprising fact that computability and quantitative error control has received little attention in the theory and practice of numerical methods for differential equations including CFD over the years starting in the 1950s these subjects have been developed, despite the clearly fundamental importance of the concepts. It is clearly essential to be able to distinguish cases with computational errors of order, e.g. 1–10 per cent from cases with large errors which cannot have any meaning. The purpose of adaptive error control is to identify accurate computations and to realize efficient use of computational resources to meet accuracy demands. The limits of computability in CFD is today largely unexplored; 3D flows with moderately large Reynolds numbers of order up to say  $10^3$  may be computable over time intervals of moderate length, while for higher Reynolds numbers, turbulence modelling of small scales is necessary to effectively reduce the Reynolds number to computable ranges. The purpose of this paper is to give some concrete information on the question of computability in CFD.

In recent work presented in monograph form in Reference 1, see also References 2–11 and references therein, we have developed a general method for adaptive error control for finite element methods for a large class of differential equations including the Navier–Stokes equations for fluid flow. The adaptive error control is based on *a posteriori* error estimates involving the

computed finite element solution, or more precisely the residual of the finite element solution. The residual is obtained inserting the computed approximate solution into the given differential equation. The *a posteriori* error estimates are based on a combination of the Galerkin orthogonality inherent in the finite element method and strong stability. Here, strong stability is the relevant stability concept coupling the error in the computed solution to the residual through a multiplicative strong stability factor denoted by  $S_1$  below. The strong stability factor  $S_1$  is estimated computationally in auxiliary computations solving an associated linearized dual problem. The computational difficulty of achieving a given accuracy is proportional to  $S_1$ . If  $S_1$  is too large, then computability cannot be realized. The computational estimate of  $S_1$ , which is built into the adaptive algorithm, is the necessary and sufficient ingredient making quantitative error control possible to realize. The adaptive method is implemented in prototype form in the code Femlab including applications to elliptic, parabolic and hyperbolic problems.

The methodology of Eriksson *et al.*<sup>1</sup> is based on Galerkin methods with piecewise polynomials in space–time. In particular, time discretization comes in two forms, continuous Galerkin cG( $q$ ) and discontinuous Galerkin dG( $q$ ) methods based on piecewise polynomials in time of order  $q$ , which are continuous or discontinuous, respectively.

In this note we first recall the basic principles of the general methodology for adaptive error control in Reference 1 in the context of an initial value problem. In particular, the role of the strong stability factor  $S_1$ , which appears as a multiplicative constant in the *a posteriori* error estimate underlying the adaptive algorithm, is made transparent. We then consider two particular applications illustrating different basic aspects: (i) the Lorenz system of ordinary differential equations<sup>11</sup> and (ii) Navier–Stokes equations for incompressible flow in three dimensions.<sup>6,8</sup> For these problems we present theoretical and computational estimates of the stability factor  $S_1$  together with results illustrating the performance of the algorithm for adaptive error control.

For the Lorenz system we present results from Reference 11 showing that in the typical case considered in the literature,  $S_1$  is of the order  $10^9$  on time intervals of the order 30 units, which is at the limit of computability with a standard workstation. We discuss briefly the possibilities opened by accurate computation over moderate time and the apparent impossibility of pointwise prediction and computation over long time.

Concerning the Navier–Stokes equations, we note that the traditional theoretical foundation in CFD gives little guide-line concerning the possible computability of the Navier–Stokes equations. The traditional error estimates (of *a priori* type) contain stability factors multiplying interpolation or consistency errors which typically are of size  $\exp(Re)$  in situations of interest, where  $Re$  is the Reynolds number, cf. Reference 12. If this was an accurate estimate, then computability would be excluded also for relatively small Reynolds numbers. This is in conflict with computational experience which strongly indicate that many flows with moderately large Reynolds numbers in the range  $10^2$ – $10^3$  in fact are computable over moderately large time intervals. Thus, the existing error analysis in CFD does not appear to reflect the nature of actual computations except possibly in the case of fully developed turbulent flow over moderately large time intervals, which does not appear to be computable.

In References 6 and 7 we have identified some basic flows for which computability indeed can be proved theoretically by showing that the stability factor  $S_1$  is proportional to  $Re$  instead of  $\exp(Re)$  on time intervals of length  $Re$ . Analogous estimates for stationary flows are given in Reference 8. These flows include almost parallel flows in different settings such as Couette flow, Poiseuille pipe flow and Taylor–Couette flow between rotating cylinders. Our corresponding error estimates (of both *a priori* and *a posteriori* type) indicate that highly organized flow such as almost parallel flow is computable for Reynolds numbers up to say order  $10^3$  over relatively long time intervals. Our error estimates appear to be sharp and to describe the actual size of the error.

In this note we present additional computational estimates of the strong stability factor  $S_1$  for driven cavity flow in three dimensions.

An outline of the paper is as follows. We first consider as a model an initial value problem for system of ordinary differential equations and prove for this case an *a posteriori* error estimate for the dG(0)-method. The proof displays in simple proto-type form the interplay between strong stability and Galerkin orthogonality. We then present computational results for the Lorenz system and the incompressible Navier–Stokes equations.

## 2. ADAPTIVE ERROR CONTROL FOR AN INITIAL VALUE PROBLEM

We shall illustrate the principle for adaptive error control for the dG(0)-method for an initial value problem of the form : Find  $u = u(t)$  such that

$$\begin{aligned} u_t + f(t, u) &= 0 \quad \text{for } t > 0 \\ u(0) &= u_0 \end{aligned} \quad (1)$$

where  $f(t, \cdot) : H \rightarrow H$  is a given vector field for  $t > 0$  with  $H$  a Hilbert space and  $u_t = du/dt$ . For simplicity, we consider the case  $H = R^d$  where  $R^d$  is Euclidean space of dimension  $d$ , but the results directly extend to infinite-dimensional systems such as the incompressible Navier–Stokes equations, see Reference 8. The dG(0)-method for (1) is defined as follows letting  $T_k$ :  $0 = t_0 < t_1 < t_2 < \dots$  be a subdivision of the time interval  $(0, \infty)$  into time intervals  $I_n = (t_{n-1}, t_n)$  of length  $k_n = t_n - t_{n-1}$  and introducing the corresponding space  $W_k$  of discontinuous piecewise constant functions on  $T_k$  with values in  $R^d$ : Find  $U \in W_k$  such that for all  $v \in [P_0(I_n)]^d$ ,  $n = 1, 2, \dots$ ,

$$\int_{I_n} (U_t + f(t, U))v dt + [U_{n-1}]v_{n-1}^+ = 0 \quad (2)$$

where  $[v_n] = (v_n^+ - v_n^-)$ ,  $v_n^\pm = \lim_{s \rightarrow \pm 0} v(t_n + s)$ ,  $U_0^- = u_0$ , and  $P_0(I_n)$  is the set of constant functions on  $I_n$ . Using the notation  $U_n \equiv U|_{I_n}$ , the dG(0)-method (2) takes the form

$$U_n - U_{n-1} + \int_{I_n} f(t, U_n) dt = 0 \quad \text{for } n = 1, 2, \dots, \quad (3)$$

where  $U_0 = u_0$ . This is a variant of the classical backward Euler method with exact evaluation of the integral with integrand  $f(t, U)$ . In case exact evaluation of this integral is not feasible, we may use quadrature for example of the form

$$\int_{I_n} f(t, U_n) dt \approx k_n f\left(\frac{t^n + t^{n+1}}{2}, U_n\right)$$

Note that the classical backward Euler method uses instead the approximation  $k_n f(t^{n+1}, U_n)$  of inferior precision at no gain of computational complexity, see Reference 13.

### 2.1. An *a posteriori* error estimate

To derive an *a posteriori* error estimate for the error  $e_N \equiv u(t_N) - U_N$  in the dG(0)-method (2) at the given time  $t_N$ ,  $N \geq 1$ , we introduce the continuous dual ‘backward’ problem

$$-\varphi_t + A(t)^* \varphi = 0 \quad \text{in } (0, t_N), \quad \varphi(t_N) = e_N \quad (4)$$

where  $A^*$  is the transpose of  $A$  and

$$A(t) \equiv \int_0^1 f'(t, su + (1-s)U) ds \quad (5)$$

so that

$$\begin{aligned} A(t)e &= \int_0^1 f'(t, su + (1-s)U) e ds \\ &= \int_0^1 \frac{d}{ds} f(t, su + (1-s)U) ds = f(t, u) - f(t, U) \end{aligned}$$

where  $f'(t, \cdot)$  is the Jacobian of  $f(t, \cdot)$ . We have integrating by parts and using the exact equation (1)

$$\begin{aligned} |e_N|^2 &= |e_N|^2 + \sum_{n=1}^N \int_{I_n} e(-\varphi_t + A^*\varphi) dt \\ &\quad \sum_{n=1}^N \int_{I_n} (e_t + A(t)e) \varphi dt + \sum_{n=1}^{N-1} [e_n] \varphi_n^+ + (u_0 - U_0^+) \varphi_0^+ \\ &= - \sum_{n=1}^N \left( \int_{I_n} (U_t + f(t, U)) \varphi dt + [U_{n-1}] \varphi_{n-1}^+ \right) \end{aligned}$$

Using now the Galerkin orthogonality (2) with  $v = \pi_k \varphi \in \mathcal{W}_k$  defined by

$$\int_{I_n} (\varphi - \pi_k \varphi) dt = 0, \quad n = 1, \dots, N$$

we obtain since  $U_t = 0$  on  $I_n$  the following error representation:

$$\begin{aligned} |e_N|^2 &= - \sum_{n=1}^N \left( \int_{I_n} (U_t + f(t, U)) (\varphi - \pi_k \varphi) dt + [U_{n-1}] (\varphi - \pi_k \varphi)_{n-1}^+ \right) \\ &= - \int_0^{t_N} f(t, U) (\varphi - \pi_k \varphi) dt - \sum_{n=0}^{N-1} [U_n] (\varphi - \pi_k \varphi)_n^+ \end{aligned}$$

Using now the easy to prove interpolation estimate

$$\left| \int_{I_n} (\varphi - \pi_k \varphi) dt \right| \leq \int_{I_n} |\varphi_t| dt$$

we see that

$$|e_N|^2 \leq \int_0^{t_N} |\varphi_t| dt \max_{n=1, \dots, N} (|[U_{n-1}]| + k_n \|f(\cdot, U_n)\|_{I_n})$$

where  $\|v\|_{I_n} = \max_{I_n} |v(t)|$ . Finally, defining the strong stability factor  $S(t_N, u, U)$  by

$$S(t_N, u, U) = \sup_{\varphi(t_N) \in R^d} \frac{\int_0^{t_N} |\varphi_t| dt}{|\varphi(t)|} \quad (6)$$

where  $\varphi$  satisfies  $-\varphi_t + A(t)^*\varphi = 0$  in  $(0, t_N)$ , we arrive at the following *a posteriori* error estimate for the parabolic model problem (1), using also the definition of  $\pi_k$  to replace  $f$  by  $f - \pi_k f$ :

*Theorem 2.1.* The solution  $U$  of the dG(0)-method (2) satisfies for  $N = 1, 2, \dots$ ,

$$|u(t_N) - U_N| \leq S(t_N, u, U) \left( \max_{n=1, \dots, N} (|U_n - U_{n-1}| + k_n \|f(\cdot, U_n) - \pi_k f(\cdot, U_n)\|_{I_n}) \right) \quad (7)$$

## 2.2. Adaptive algorithm

Based on (7) we formulate the following adaptive algorithm for controlling the error  $e(t_N)$  on the given tolerance level  $\text{TOL} > 0$ : Determine for  $n = 1, 2, \dots, N$  the timesteps  $k_n$  such that

$$S(t_N, u, U) (|U_n - U_{n-1}| + k_n \|f(\cdot, U_n) - \pi_k f(\cdot, U_n)\|_{I_n}) = \text{TOL}$$

In practice the strong stability factor  $S(t_N, u, U)$  is estimated solving the linearized dual problem (4) numerically replacing the unknown exact solution  $u$  appearing in the definition of  $A(t)$  by a computed approximate solution. The initial data  $\varphi(t_N)$  may be chosen in different ways, one possibility being the difference between two computed solutions with different tolerances, see References 10 and 11. To control the error  $e(t_N)$  to the tolerance  $\text{TOL}$  for  $N = 1, 2, \dots, M$ , the time steps are chosen so that

$$S_M(U) (|U_n - U_{n-1}| + k_n \|f(\cdot, U_n) - \pi_k f(\cdot, U_n)\|_{I_n}) = \text{TOL}, \quad n = 1, 2, \dots, M$$

where  $S_M(U) = \max_{N=1, 2, \dots, M} S(t_N, U, U)$ . The implicit nature of this algorithm with  $U$  depending on the  $k_n$  is typically handled solving the discrete problems two times over the entire time interval  $(0, t_M)$ , see e.g. Reference 11 for details.

We now present results for the Lorenz system from Reference 11 obtained applying the dG(1) in adaptive form analogous to that just presented for dG(0).

## 3. COMPUTABILITY OF THE LORENZ SYSTEM

The Lorenz system is the following three-dimensional system of ordinary differential equations:

$$\begin{aligned} \dot{x} &= -\sigma x + \sigma y \\ \dot{y} &= -rx - y - xz \\ \dot{z} &= -bz + xy \end{aligned} \quad (8)$$

$$x(0) = x_0, y(0) = y_0, z(0) = z_0$$

where  $\sigma, r$ , and  $b$  are positive constants and  $(x_0, y_0, z_0)$  is a given initial condition. This system was originally derived from a coarse spectral approximation of the Benard problem for incompressible flow and is considered to reflect properties of the flow models of meteorology. We consider the Lorenz system in the standard case with  $\sigma = 10$ ,  $b = \frac{8}{3}$ , and  $r = 28$ . System (8) then has a hyperbolic fixed point at  $(0, 0, 0)$  with one-dimensional unstable manifold, and two hyperbolic fixed points at  $(x, y, z) = (\pm 6\sqrt{2}, \pm 6\sqrt{2}, 27)$  with one-dimensional stable manifolds. In Figure 1, we present two views of a typical trajectory starting at  $(1, 0, 0)$  computed with an absolute error tolerance of 0.5 in the Euclidean norm on the time interval  $[0, 30]$ . Generic solutions started near  $(0, 0, 0)$  are repelled and end up revolving around the two non-zero fixed points, changing from one to the other with a seemingly random number of revolutions around each fixed point.

More precisely, Figure 1 indicates that the attractor consists, roughly speaking, of two 'lobes' in which the orbits around the non-zero fixed points are located. In each lobe, the spiraling segments of the trajectory seem to be grouped in 'bands' that are made up of parts of the trajectory that are

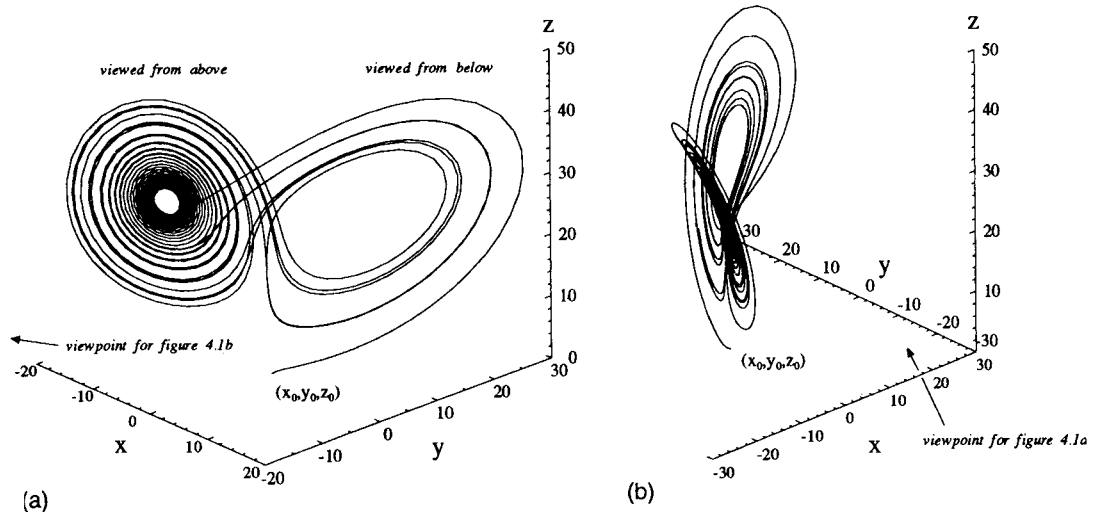


Figure 1.  $(x_0, y_0, z_0) = (1, 0, 0)$ , final time = 30 absolute error tolerance = 0.5.

spiralling out from the fixed point and parts of the trajectory that have just crossed over from the other lobe. Only the trajectories in the outer band switch to the other fixed point. This causes a sharp separation between trajectories located in the outer band and those located in the next band inside as the trajectories approach the  $z$ -axis (cutting). The trajectories in the outer band expand in width as they approach the other fixed point, with trajectories near the outside of the band ending up nearer to the fixed point (expansion and flipping). Finally, trajectories approaching one lobe, quickly get interlaced with the trajectories already spiralling in the lobe. In short, we can describe the dynamics of the Lorenz system as a never-ending process of cutting, expansion, flipping and interlacing. The cutting and expansion clearly introduces a strong sensitivity to perturbations making both prediction or computation over long time impossible. Questions concerning the long-time behaviour of the Lorenz system in a pointwise sense, or the more precise nature of the so-called 'strange attractors' therefore seem impossible to answer by computation (and probably also by theoretical means). Accurate computation over finite time, on the other hand, has the potential of supplying a wealth of information on the nature of solutions of the Lorenz system. For more details, see Reference 11.

In the literature, the Lorenz system is typically considered to be computable only on very short time intervals. For example, the standard 'worst-case' estimate limits the computability to less than one time unit. We are able to obtain an accurate computation over 30 time units because though the Lorenz system is data sensitive, the error actually grows much more slowly than indicated by a crude worst case *a priori* estimate. In Figure 2, we plot the stability factor  $S_1(t, u)$  computed every 0.5 time units for a typical solution  $u = (x, y, z)$ . Note that  $S_1$  grows with time, but not monotonically, and that  $S_1$  is of order  $10^9$  for  $t = 30$ , which time the error control is lost.

To evaluate the reliability of the adaptive error control, we performed the following experiment: Using the initial data  $(-8.05, -9.35, 25.6)$ , we computed with residual tolerances of  $10^{-5}$  and  $10^{-9}$ . We then computed an approximate error by taking the difference between the more accurate and the less accurate solution. In Figure 3(a), we plot the approximate error computed this way and the computed error from the adaptive computation with the coarse tolerance  $10^{-5}$ . We note a close comparison between the computed and the approximate error.

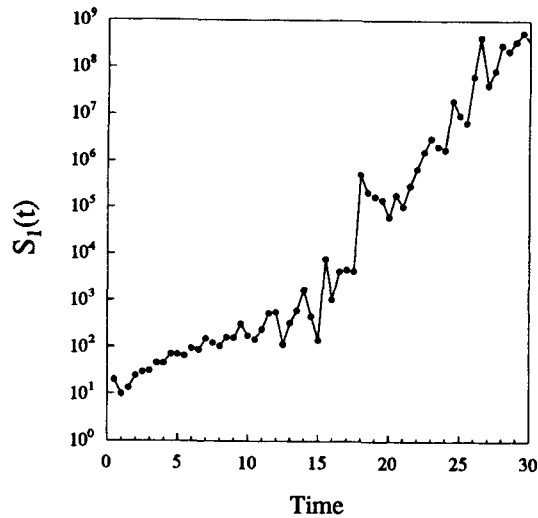


Figure 2.  $(x_0, y_0, z_0) = (1, 0, 0)$ , absolute error tolerance = 0.5

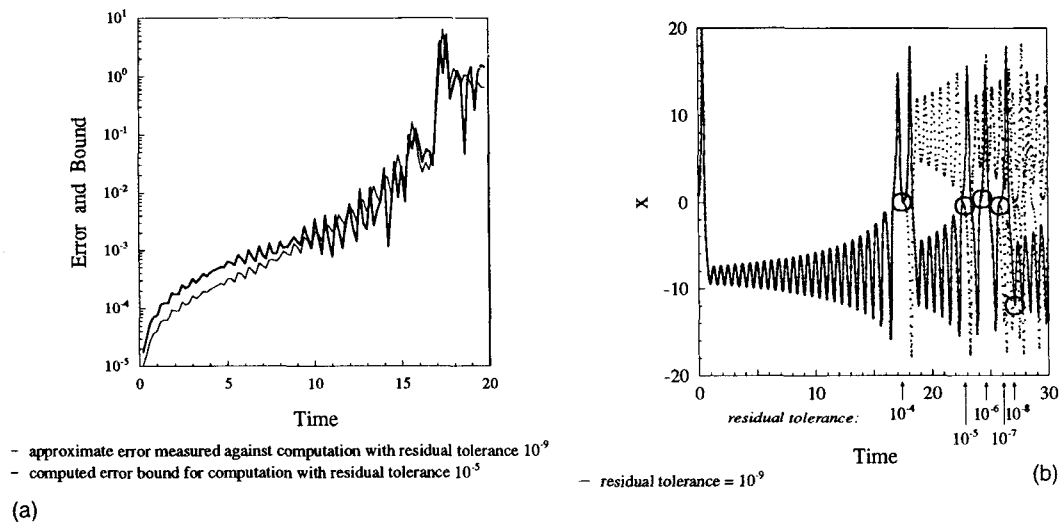


Figure 3. (---) approximate error measured against computation with residual tolerance  $10^{-9}$ , (—) computed error bound for computation with residual tolerance  $10^{-5}$ . Initial data: (a)  $(x_0, y_0, z_0) = (-8.05, -9.35, 25.6)$ . (b) Computation with decreasing residual tolerance (—) residual tolerance =  $10^{-9}$ ,  $(x_0, y_0, z_0) = (1, 0, 0)$

We obtained similar results for a variety of initial data. In Figure 3(b), we plot the  $x$  component of computations made with decreasing residual tolerances. We have indicated the points in time at which the successive computations with decreasing tolerances diverge from the correct solution. The presented results strongly indicate that indeed the adaptive error control performs as desired.

To give some idea of the behaviour of the time step control, we plot the time steps used in a computation with absolute error tolerance 0.75 in Figure 4(a). The step sizes vary roughly by a factor of 6 over the total interval of computation. In Figure 4(b), we plot the residual errors for

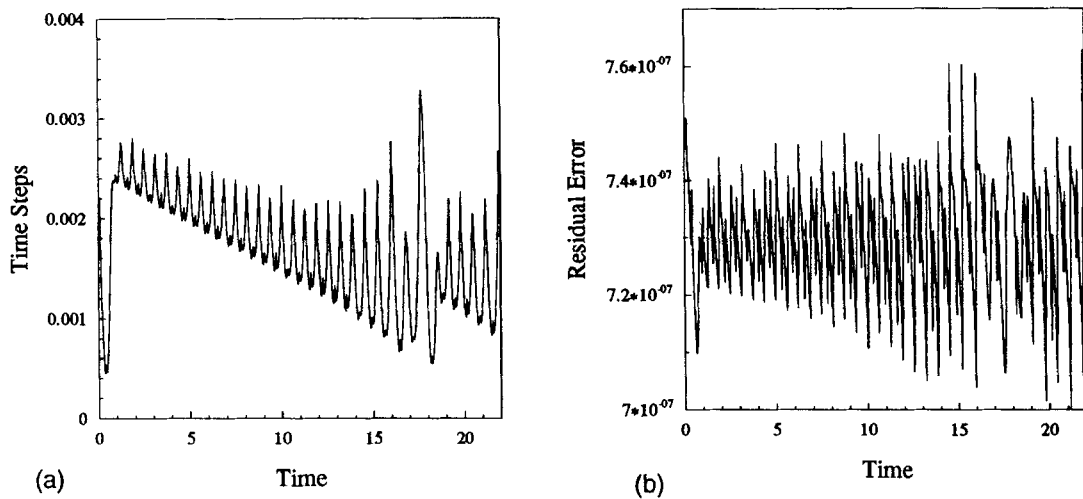
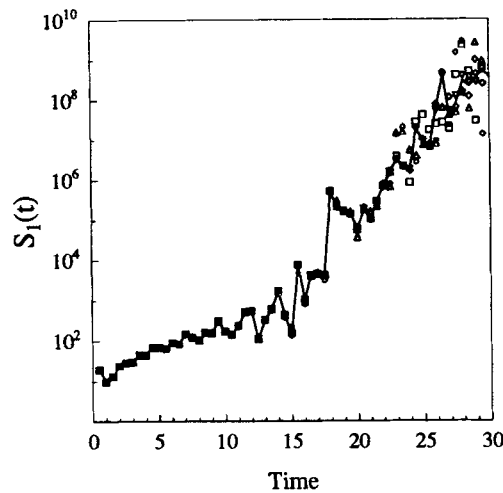


Figure 4. (a)  $(x_0, y_0, z_0) = (1, 0, 0)$ , absolute error tolerance = 0.75, (b) residual errors



residual tolerance:

•  $10^{-4}$      $\Delta$   $10^{-5}$      $\square$   $10^{-6}$      $\diamond$   $10^{-7}$      $\nabla$   $10^{-8}$      $+$   $10^{-9}$

Figure 5.  $S_1(t)$  computed for various tolerances  $(x_0, y_0, z_0) = (1, 0, 0)$

this computation. We note that these values are kept within 10 per cent of a constant value. With more computational work, the size of the variations can be reduced, which produces a more smoothly varying error bound.

To give some idea of the accuracy of the computed stability factors, we plot  $S_1(t)$  computed for various tolerances in Figure 5. As indicated in Figure 3(b), the trajectories agree up to time 17, then begin to diverge one by one from the most accurate trajectory. In the time period  $[0, 17]$ , the



value of  $S_1(t)$  is essentially the same for all computations. On the whole interval, we see that the magnitude of the stability factors is relatively insensitive to the particular trajectory used in the linearization. Of course, there is some local variation since at any given moment, some trajectories are orbiting a non-zero fixed point while others are crossing over from one nonzero fixed point to the other.

#### 4. COMPUTABILITY OF THE INCOMPRESSIBLE NAVIER-STOKES EQUATIONS

##### 4.1. General remarks

Existing error estimates for the non-stationary Navier–Stokes equations over relevant time scales, typically involve estimates of stability factors of the order  $\exp(Re)$ , where  $Re$  is the Reynolds number. If these estimates would reflect actual stability properties, fluid flow would only be computable for Reynolds numbers up to say 10. This contradicts computational practice which indicates computability of several flows of moderate Reynolds numbers of order up to  $10^3$ – $10^4$ . In References 6 and 7 we have identified certain model flows related to almost parallel flow where the strong stability factor can be theoretically estimated by instead  $C Re$  with a relatively small proportionality constant  $C$ . Computational results supporting these estimates indicating that  $C \sim 0.02$  for Pouiseuille flow between two plates (with a somewhat differently defined stability factor), are given in Reference 14. These results indicate that error control for certain flows of moderate Reynolds number of order say  $10^2$ – $10^4$  may be possible to achieve.

For the stationary Navier–Stokes equations the situation is analogous. The existing error analysis does not include accurate estimates of stability factors. The current standard in theoretical analysis is simply to assume a certain stability estimate involving a completely unspecified constant, see e.g. References 12. This results in an error analysis without any quantitative aspect, which may have little meaning in a particular application. In Reference 8 we have identified some cases related to almost parallel flow for which it is possible to prove theoretically that the strong stability factor is again proportional to the Reynolds number, showing computability of such flows for moderate Reynolds numbers.

To illustrate the general principles of adaptive error control we derive below an *a posteriori* error estimate for the stationary Navier–Stokes equations. We also present computational estimates of the strong stability factor  $S_1$  for driven cavity flow in three dimensions for Reynolds numbers in the range  $10^2$ – $10^3$ .

It is important to note that the stability properties of the Navier–Stokes equations in 2D and 3D may be vastly different, see e.g. References 6 and 15. Since real fluid flow is three-dimensional, only computations in 3D can reflect the stability properties real fluid flow. This is in particular important in transition to turbulence where a full 2D computation may be incapable of capturing the essential 3D nature of the transition process, see References 6 and 7.

##### 4.2. The stationary Navier–Stokes equations

The stationary incompressible Navier–Stokes equations read: Find  $(u, p)$  such that

$$\begin{aligned} (u \cdot \nabla)u - \nu \Delta u + \nabla p &= f \quad \text{in } \Omega \\ \nabla \cdot u &= 0 \quad \text{in } \Omega \\ u &= 0 \quad \text{on } \partial\Omega \end{aligned} \tag{9}$$

where  $u = (u_1, u_2, u_3)$  and  $p$  are the velocity and the pressure of a Newtonian fluid with viscosity  $\nu > 0$ , enclosed in the volume  $\Omega$  in  $\mathbf{R}^3$ , and  $f$  is a given driving force. We assume that (9) is normalized, without loss of generality, so that the 'reference' velocity  $U$  and length scale  $L$  are both equal to one. The Reynolds number  $Re$  is then by definition given by  $Re = UL\nu^{-1} = \nu^{-1}$  (where  $\nu$  is to be understood as a dimensionless quantity). We consider here the case with  $Re$  moderately large, say in the range  $10$ – $10^4$ , in which case (9) may be expected to have a physically significant stationary solution under suitable conditions on the data.

Introducing the space  $\hat{V} = V \times H$ , where  $V = H_0^1[(\Omega)]^3$  and  $H = L_2(\Omega)/\mathbf{R}$ , we give the problem (9) the following variational formulation: Find  $\hat{u} \equiv (u, p) \in \hat{V}$  such that

$$A(u; \hat{u}, \hat{v}) = L(v) \quad \forall \hat{v} \equiv (v, q) \in \hat{V} \quad (10)$$

where, with  $\hat{w} = (w, r)$ ,

$$\begin{aligned} A(u; \hat{w}, \hat{v}) &= a(w, v) + b(u; w, v) - (r, \nabla \cdot v) + (q, \nabla \cdot w) \\ b(u; w, v) &= \int_{\Omega} (u \cdot \nabla) w \cdot v \, dx \\ a(w, v) &= \nu \int_{\Omega} \sum_{i=1}^3 \nabla w_i \cdot \nabla v_i \, d\bar{x}, \quad L(v) = (f, v) \equiv \int_{\Omega} f \cdot v \, dx \end{aligned}$$

We denote below by  $\|\cdot\|$  the  $[L_2(\Omega)]^3$ -norm.

#### 4.3. Finite element approximation

To formulate a finite element method for (9), let  $V_h$  and  $H_h$  be finite-dimensional subspaces of  $V$  and  $H$  consisting of continuous piecewise polynomials on a triangulation  $T_h = \{K\}$  of  $\Omega$  into elements  $K$  of diameter  $h_K$  given by the mesh function  $h(x) = h_K$  for  $x \in K$ . For simplicity we assume that the pair  $(V_h, H_h)$  satisfies a usual Babuska–Brezzi condition. We recall that with least-squares stabilizations, the spaces  $V_h$  and  $H_h$  may alternatively be chosen independently, for instance equal order continuous approximations. For definiteness, we assume that  $V_h$  contains piecewise linears and  $H_h$  piecewise constants.

We consider the following standard Galerkin finite element method for (10): Find  $\hat{u}_h = (u_h, p_h) \in \hat{V}_h \equiv (V_h, H_h)$ , such that

$$A(u_h; \hat{u}_h, \hat{v}) = F(v) \quad \forall \hat{v} = (v, q) \in \hat{V}_h \quad (11)$$

#### 4.4. A posteriori error estimate

We shall now prove an *a posteriori* error estimate for (11) following an approach analogous to that used above involving the following steps:

- (1) Error representation via a linearized dual continuous problem.
- (2) Use of the Galerkin orthogonality.
- (3) Interpolation error estimates for the dual solution.
- (4) Strong stability for the dual continuous problem.

We represent the error  $e = u - u_h$ , through the solution  $\hat{\phi} \equiv (\phi, \chi)$  of the following dual linearized problem: Find  $\hat{\phi} \in \hat{V}$ , such that

$$L(u, u_h; \hat{v}, \hat{\phi}) = (v, \kappa) \quad \forall \hat{v} \in \hat{V} \quad (12)$$

where  $\kappa = e$ , and

$$L(u, U; \hat{v}, \hat{\phi}) = -((u \cdot \nabla)\phi - \nabla U \cdot \phi, v) + a(\phi, v) + (\nabla \chi, v) - (\nabla q, \phi). \quad (13)$$

Note that  $L(u, U; \cdot, \cdot)$  represents the dual linearized Navier–Stokes equations linearized ‘between’  $u$  and  $U$  so that

$$A(u; \hat{u}, \hat{\phi}) - A(U; \hat{U}, \hat{\phi}) = L(u, U; \hat{e}, \hat{\phi}).$$

Choosing now  $v = e$  in (12) and integrating by parts gives

$$\begin{aligned} \|e\|^2 &= L(u, U; \hat{e}, \hat{\phi}) = A(u; \hat{u}, \hat{\phi}) - A(U; \hat{U}, \hat{\phi}) \\ &= F(\hat{\phi}) - A(U; \hat{U}, \hat{\phi}) = F(\hat{\phi} - \hat{\phi}^h) - A(U; \hat{U}, \hat{\phi} - \hat{\phi}^h) \\ &= ((U \cdot \nabla)U - f + \nabla p_h, \phi - \phi^h) + (v \nabla U, \nabla(\phi - \phi^h)) + (\nabla \cdot U, \chi - \chi^h) \end{aligned}$$

where  $\hat{\phi}^h = (\phi^h, \chi^h) \in \hat{V}_h$  is a nodal interpolant of  $\hat{\phi}$ .

We now define the strong stability factor  $S_1(u, U)$  to be the smallest constant satisfying

$$\|\nabla \chi\| + \|v D^2 \phi\| \leq S_1(u, U) \|\kappa\| \quad \forall \kappa \in L_2(\Omega)$$

where  $\hat{\phi}$  satisfies (12). Using this definition together with relevant interpolation estimates for  $\hat{\phi} - \hat{\phi}^h$  in particular of the form

$$\|\phi - \phi_h\| \leq C^i \|h^2 D^2 \phi\|$$

where  $D^2 v$  denotes the second derivative of  $v$  of maximal modulus, we now obtain the following *a posteriori* error estimate, see References 1 and 3 for more details.

*Theorem 4.1.* Let  $u$  and  $U$  be the solutions of the exact and discrete Navier–Stokes equations (9) and (11). Then

$$\|u - u_h\| \leq C^i S_1(u, U) (\|v^{-1} h^2 R_1(U)\| + \|h R_2(U)\|) \quad (15)$$

where

$$\begin{aligned} R_1(U)|_K &= |(U \cdot \nabla) U p_h - v \Delta U - f| + |v D_h^2 U| \quad \text{on } K \\ R_2(U) &= |\nabla \cdot U| \end{aligned}$$

Here

$$D_h^2 v = \frac{1}{2} \max_{S \in \partial K} \left| \left[ \frac{\partial v}{\partial n_S} \right] \right| h_K^{-1} \quad \text{on } K$$

where  $[\partial v / \partial n_S]$  is the jump in normal derivative  $\partial v / \partial n_S$  across the side  $S$  of the element  $K \in T_h$ .

The crucial question is now the size of the stability factor  $S_1(u, U)$ . In Reference 8 we proved for a model problem of nearly parallel streamwise constant pipe flow that  $S_1 \sim Re$  an estimate which appears to be sharp in the dependence on  $Re$ , see also Reference 14. The proof is based on simple ‘energy’ estimates using the decoupled nature of the linearized problem in the case of nearly parallel flow.

#### 4.5. Computational estimates of $S_1$ for the driven cavity flow

We have computed approximations of the strong stability factor  $S_1$  for the 3D driven cavity flow in a box of side 1 with the tangential fluid velocity equal to one on the top of the box. For Reynolds numbers 100, 200, 300, 400, 500, 600 and 700, we obtained the following values of

$S_1$ : 1.48, 1.60, 1.60, 1.60, 1.56, 1.55, 1.50. The corresponding estimated relative  $L_2$  errors in the velocity were 0.15, 0.27, 0.38, 0.48, 0.58, 0.69, 0.80 using adapted meshes with approximately 2200 nodes and piecewise linear approximation. For Reynolds numbers up to 700 the strong stability factors seems to be of moderate size indicating computability in this range. The presented results are preliminary and will be followed by extensive numerical experiments to be published elsewhere.

## 5. CONCLUSION

We have presented some basic features of adaptive error control. Adaptive algorithms for quantitative error control for finite element methods may be designed in large generality including fluid flow by combining Galerkin orthogonality and strong stability. The estimates include a strong stability factor  $S_1$  which is estimated computationally solving an associated linearized dual problem. The computational difficulty of a given problem is proportional  $S_1$ . A certain class of problems in CFD with moderately large Reynolds numbers appears to be computable because  $S_1$  is of moderate size. For larger Reynolds numbers,  $S_1$  may become so large that computability is not realized. In these cases turbulence modelling is necessary to effectively reduce the Reynolds number to computable ranges. Accurate computation over finite time in massive benchmark calculations may open possibilities of designing and evaluating turbulence models to be used in production runs requiring less massive computational effort.

## REFERENCES

1. K. Eriksson, D. Estep, P. Hansbo and C. Johnson, *Adaptive Finite Element Methods*, North-Holland, Amsterdam, to appear.
2. C. Johnson, 'Adaptive finite element methods for diffusion and convection problems', *Comput. Methods Appl. Mech. Eng.*, **82**, 301–332 (1990).
3. K. Eriksson and C. Johnson, 'Adaptive finite element methods for parabolic problems I: a linear model problem', *SIAM J. Numer. Anal.*, **28**, 43–77 (1991).
4. K. Eriksson and C. Johnson, 'Adaptive streamline diffusion finite element methods for stationary convection–diffusion problems', *Math. Comp.*, **60**, 167–188 (1993).
5. C. Johnson and P. Hansbo, Adaptive finite element methods in computational mechanics, *Comput. Methods Appl. Mech. Eng.*, **101**, 143–181 (1992).
6. C. Johnson, R. Rannacher and M. Boman, 'Numerical and hydrodynamic stability: towards error control in CFD', *SIAM J. Numer. Anal.*, to appear.
7. C. Johnson, R. Rannacher and M. Boman, 'On transition to turbulence and error control in CFD', Preprint 1994–26, Mathematics Dept., Chalmers University of Technology.
8. C. Johnson and R. Rannacher, 'On error control in CFD', Notes on Numerical Fluid Mechanics, Vol. 47 eds. Hebekker, Rannacher, Wittum, Vieweg, 1994.
9. C. Johnson and A. Szepessy, 'Adaptive finite element methods for conservation', *CPAM*, to appear.
10. D. Estep, 'A posteriori error bounds and global error control for approximations of ordinary differential equations', *SIAM J. Numer. Anal.*, to appear.
11. D. Estep and C. Johnson, 'The computability of the Lorenz system', Preprint, Mathematics Dept., Chalmers University of Technology 1994.
12. V. Girault and P. A. Raviart, *Finite Element Methods for the Navier–Stokes Equations*, Lecture Notes in Math., Vol. 749, Springer, Berlin, 1979.
13. K. Eriksson and C. Johnson, 'Adaptive finite element methods for parabolic problems V: long time integration', *SIAM J. Numer. Anal.*, to appear.
14. N. Eriksson, 'On the stability of pipe flow', *Master of Science Thesis*, Mathematics Dept. Chalmers University of Technology, 1993.
15. L. N. Trefethen, A. E. Trefethen, S. C. Reddy and T. A. Driscoll, 'A new direction in hydrodynamic stability: beyond eigenvalues', *Technical Report CTC92TR115 12/92*, Cornell Theory Center, Cornell University, 1992.